RADIOPHYSICS

Original article
DOI: https://doi.org/10.18721/JPM.18115

A COHERENT DOUBLE SPECTRAL METHOD FOR MEASURING THE PARAMETERS OF SINGLE-MODE OPTICAL FIBERS WITH STRONG LINEAR BIREFRINGENCE

A. I. Golovchenko[1], *A. V. Petrov*[1], *V. S. Temkina*[1], *A. B. Archelkov*[1], *M. K. Tsibinogina*[1], *O. I. Kotov*[1]✉

[1] Peter the Great St. Petersburg Polytechnic University, St. Petersburg, Russia;

[2] Concern CSRI Elektropribor, JSC, St. Petersburg, Russia

✉ kotov@rphf.spbstu.ru

Abstract. In this work, a coherent spectral method for measuring the parameters of anisotropic optical fiber with taking into account polarization dispersion of refractive indices (RI) and possible angular mismatches of birefringence axes of the circuit optical elements has been analyzed thoroughly. Using the Jones matrix method, the measuring polarization interferometer was treated and the relationship between its characteristics and circuit parameters was obtained. The deviations of the axial angles from the optimal ones were shown to lead to a decrease in the contrast of the output interference signals and to the appearance of parasitic spectral components. Analytical expressions for the birefringence and beat length of polarization modes having regard to the RI dispersion, as well as for the spectral transfer function (STF) of the polarization interferometer and its Fourier image were derived. The features of the application of the described method for measuring the key parameters of three types of birefringent fibers were experimentally demonstrated.

Keywords: polarization of light, Jones vector, polarization mode, anisotropic light guide

Funding: The reported study was funded by Russian Science Foundation (Grant No. 23-72-01101). https://rscf.ru/project/23-72-01101/.

Citation: Golovchenko A. I., Petrov A. V., Temkina V. S., Archelkov A. B., Tsibinogina M. K., Kotov O. I., A coherent double spectral method for measuring the parameters of single-mode optical fibers with strong linear birefringence, St. Petersburg State Polytechnical University Journal. Physics and Mathematics. 18 (1) (2025) 182–200. DOI: https://doi.org/10.18721/JPM.18115

Научная статья
УДК 535.5, 535-4, 535.012.2
DOI: https://doi.org/10.18721/JPM.18115

КОГЕРЕНТНЫЙ ДВОЙНОЙ СПЕКТРАЛЬНЫЙ МЕТОД ИЗМЕРЕНИЯ ПАРАМЕТРОВ ОДНОМОДОВЫХ ВОЛОКОННЫХ СВЕТОВОДОВ С СИЛЬНЫМ ЛИНЕЙНЫМ ДВУЛУЧЕПРЕЛОМЛЕНИЕМ

А. И. Головченко[1], *А. В. Петров*[1], *В. С. Темкина*[1], *А. Б. Арчелков*[1], *М. К. Цибиногина*[2], *О. И. Котов*[1]✉

[1] Санкт-Петербургский политехнический университет Петра Великого, Санкт-Петербург, Россия;

[2] ОАО, «Концерн «ЦНИИ «Электроприбор», Санкт-Петербург, Россия

✉ kotov@rphf.spbstu.ru

Аннотация. В работе детально проанализирован когерентный спектральный метод измерения параметров анизотропных волоконных световодов с учетом поляризационной дисперсии показателей преломления (ПП) и возможных угловых рассогласований осей двулучепреломления оптических элементов схемы. С использованием метода матриц Джонса рассмотрен измерительный поляризационный интерферометр и найдены зависимости его характеристик от параметров схемы. Показано, что отклонения величин осевых углов от оптимальных приводит к снижению контраста выходных интерференционных сигналов и появлению паразитных спектральных составляющих. Получены аналитические выражения для двулучепреломления и длины биений поляризационных мод с учетом дисперсии ПП, а также для спектральной передаточной функции поляризационного интерферометра и ее Фурье-образа. Экспериментально продемонстрированы особенности применения описанного метода для измерения ключевых параметров двулучепреломляющих волоконных световодов трех типов.

Ключевые слова: поляризация света, вектор Джонса, поляризационная мода, длина биений мод, анизотропный световод

Финансирование: Исследование выполнено за счет гранта Российского научного фонда № 01101-72-23, https://rscf.ru/project/23-72-01101/.

Ссылка для цитирования: Головченко А. И., Петров А. В., Темкина В. С., Арчелков А. Б., Цибиногина М. К., Котов О. И. Когерентный двойной спектральный метод измерения параметров одномодовых волоконных световодов с сильным линейным двулучепреломлением // Научно-технические ведомости СПбГПУ. Физико-математические науки. 2025. Т. 18. № 1. С. 182–200. DOI: https://doi.org/10.18721/JPM.18115

Introduction

Optical fibers with strong linear birefringence, belong to a special class of single-mode optical fibers that have the property of maintaining the linear state of polarization in light waves propagating through them (also called polarization-maintaining (PM) fibers). These fibers are widely used in optical systems requiring polarization matching of interfering waves: in coherent optical fiber communication systems [1, 2], in fiber-optic sensors [3] and in information processing devices [4–8]. The practical parameters of such optical fibers, which make it possible to evaluate their capability to maintain the state of linear polarization, are birefringence and the beat length of polarization modes [9].

Linear birefringence is determined by the difference in refractive indices $B = n_x - n_y$ of two orthogonal, linearly polarized waves whose electric field vectors are oriented along the x and y axes (the so-called polarization modes). As a rule, the birefringence value is found by measuring the beat length of polarization modes $L_b = \lambda/B$.

The beat length of these modes is the distance at which the difference in their phase delay reaches 2π. The beat length can be measured if the light propagating inside the fiber is exposed to phase modulation. Phase modulators [10] can be used for this purpose, as well as devices applying transverse force [11], heating or elongation of the fiber [3].

Another well-known approach to phase modulation is the spectral method, analyzing the radiation transmitted through the PM fiber while scanning the frequency of optical radiation.

There are two modifications of this method:

coherent (using a laser);

incoherent (using a superluminescent LED and an optical spectrum analyzer).

With both approaches, the interference signal of polarization modes of this fiber is recorded at the output of the optical circuit with PM fiber. The magnitude of this signal varies with modulation in the phase difference of the polarization modes as a result of optical frequency scanning. It should be noted that in the case of linear phase modulation, the corresponding signal is harmonic. In both cases, the beat length can be estimated by measuring the period of the interference signal with wavelength-modulated light

There are other approaches to measuring birefringence, for example, based on light backscattering [12–14].

Spectral methods have become widespread [15] as electronic components and fiber technologies for optical information systems are further developed. Continuous-wave laser devices with high coherence and a wide range of spectral tuning have been constructed [16]. Side-hole single-mode fibers with birefringence of the order of 10^{-4} have gained popularity in fiber-optic sensors for measuring hydrostatic pressure and elongation [17, 18].

Efforts are underway to improve the parameters of both PM fibers [19] and methods for measuring their characteristics [11, 20, 21]. The advantage of this approach is that it provides linear scanning of the radiation phase in a wide range without resorting to traditional optical modulators, which expands the scope of its application and increases the accuracy of measurements.

The parameters of PM fiber were measured earlier in [15] by excitation of a single-mode polarization interferometer (SMPI) by an incoherent LED source; the period of the received interference signal was measured with an optical spectrum analyzer. However, as we intend to prove in this paper, in practice, the waveform of the given signal may deviate from a harmonic, due to mismatch between the birefringence axes of the fiber and the axes of the input and output fibers. In this case, direct measurement of the period of the interference signal may produce inaccurate results.

In this paper, it is proposed to use double spectral transformation of SMPI signals:

the first transformation is to find the optical transmission spectrum of a polarization interferometer, the so-called spectral transfer function (STF);

the second transformation is the spectral Fourier transform of interference signals forming the SPF.

This double transformation makes it possible to correctly determine the frequency and period of the low-frequency spectral component of the Fourier transform corresponding to the interference of the principal polarization modes. This approach can reduce the error level in measurements of the period of the interference signal and, accordingly, the beat length of the polarization modes associated with possible angular mismatches of the elements in the SMPI circuit.

We previously used a similar method of double spectral transformation to measure the parameters of an intermodal fiber interferometer in both coherent and incoherent configurations [22, 23]. However, as discussed below, applying this method to PM fibers has its own peculiarities.

Here, we analyze a fully fiber-based configuration of a polarization interferometer without using any volumetric optical elements. The paper presents a model describing this approach and taking into account possible angular mismatches of individual elements of the optical circuit in their connections, distorting the measurement results.

We accounted for dispersion of refractive indices of orthogonal polarization modes. This issue has been considered in numerous earlier studies [15, 24–26]. We obtained analytical expressions

for the STF in the SMPI, characterizing the effect of dispersion on the key parameters of PM fibers: the beat length of the polarization modes and birefringence.

The paper reports on numerical simulation of various characteristics of a polarization interferometer, such as the STF and its Fourier transform, the birefringence, and the beat length of polarization modes. We conducted experiments to measure the parameters of various types of PM fibers, yielding good agreement with theoretical models and proving that this approach can be used for accurate measurements of parameters of fiber optical fibers with linear birefringence.

Theoretical analysis

Single-fiber polarization interferometer. To implement the method for measuring birefringence considered in this paper, the fiber under study is incorporated into the circuit of a single-fiber polarization interferometer (SFPI) [15] (Fig. 1).

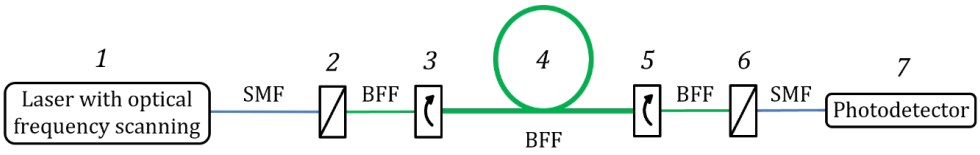

Fig. 1. Circuit of single-fiber polarization interferometer (SFPI):
laser *1* with optical frequency scanning; fiber polarizer *2*; fusion splicings *3*, *5*; fiber *4*; fiber polarizer *6*; photodetector *7*; single-mode fiber (SMF), birefringent fiber (BFF)

Laser *1* emits light whose wavelength is scanned in a certain range:

$$\lambda_0 - 0.5\cdot\Delta\lambda_{span};\ \lambda_0 + 0.5\cdot\Delta\lambda_{span}.$$

After passing through polarizer *2*, linearly polarized light propagates along one of the axes of the PM fiber aligned with the polarizer. To excite two polarization modes in the fiber, it is necessary that the axes of the fiber be oriented at an angle of 45° relative to the polarization direction of the light at the output of polarizer *2*. In our study, this was achieved during splicing of the fiber with the fiber inputs using a device capable of detecting and aligning the birefringence axes with the given angles (splices *3* and *5*). After passing through the fiber and splicings *5*, two orthogonal polarization modes are formed in the output PM fiber, each arising from the interference of two polarization modes excited in the fiber. One of the polarization modes in the output fiber is completely suppressed by polarizer *6*, after which the interference signal is received by photodetector *7*.

To analyze the processes in the SFPI circuit, it is most convenient to use the Jones matrix method [27, 28]. Let us briefly overview our measuring circuit.

The Jones vector at the output of the first polarizer is written as:

$$\mathbf{E}_{in} = \begin{pmatrix} 0 \\ 1 \end{pmatrix}. \tag{1}$$

We assume that polarizer *6* at the output of the circuit is oriented parallel to input polarizer *2*. In this case, the corresponding matrix can be written as

$$P_2 = \begin{pmatrix} 0 & 0 \\ 0 & 1 \end{pmatrix}. \tag{2}$$

Fusion splicings *3* and *5* for the case of orientation at angles $\psi_{1,2} = 45°$ can be represented by the following rotation matrix:

$$R_{1,2}(\psi_{1,2}) = \begin{pmatrix} \cos\psi_{1,2} & \sin\psi_{1,2} \\ -\sin\psi_{1,2} & \cos\psi_{1,2} \end{pmatrix} = \frac{1}{\sqrt{2}}\begin{pmatrix} 1 & 1 \\ -1 & 1 \end{pmatrix}. \tag{3}$$

PM fiber *4* is described by the following matrix:

$$W_0 = \begin{pmatrix} \exp[-i\beta_x(\lambda)\cdot L] & 0 \\ 0 & \exp[-i\beta_y(\lambda)\cdot L] \end{pmatrix}, \tag{4}$$

where L is the length of the fiber considered; $\beta_{x,y}(\lambda)$ are the propagation constants of orthogonal polarization modes (these are functions of the wavelength λ, as written).

We emphasize that matrix (4) is presented for the case when the amplitudes of polarization modes are equal.

The dependence of propagation constants $\beta_{x,y}(\lambda)$ on the wavelength is of fundamental importance for further analysis. However, we use a more compact notation $\beta_{x,y}$, implying this dependence.

Thus, taking into account expressions (2)–(4), we can write the complete Jones matrix for the measuring circuit:

$$\begin{gathered} W_\Sigma = P_2 \cdot R_2(\psi_2)\cdot W_0 \cdot R_1(\psi_1) = \\ = \begin{pmatrix} 0 & 0 \\ 0 & 1 \end{pmatrix} \cdot \frac{1}{\sqrt{2}} \begin{pmatrix} 1 & 1 \\ -1 & 1 \end{pmatrix} \cdot \begin{pmatrix} e^{-i\beta_x L} & 0 \\ 0 & e^{-i\beta_y L} \end{pmatrix} \cdot \frac{1}{\sqrt{2}} \begin{pmatrix} 1 & -1 \\ 1 & 1 \end{pmatrix} = \\ = \frac{1}{2} \begin{pmatrix} 0 & 0 \\ -e^{-i\beta_x L} + e^{-i\beta_y L} & e^{-i\beta_x L} + e^{-i\beta_y L} \end{pmatrix}. \end{gathered} \tag{5}$$

In view of expressions (1) and (5), the Jones vector at the output of the SFPI can be written as follows:

$$\mathbf{E}_{out} = W_\Sigma \cdot \mathbf{E}_{in} = \frac{1}{2} \begin{pmatrix} 0 & 0 \\ -e^{-i\beta_x L} + e^{-i\beta_y L} & e^{-i\beta_x L} + e^{-i\beta_y L} \end{pmatrix} \cdot \begin{pmatrix} 0 \\ 1 \end{pmatrix} = \frac{1}{2} \begin{pmatrix} 0 \\ e^{-i\beta_x L} + e^{-i\beta_y L} \end{pmatrix}. \tag{6}$$

Then the light intensity at the output of the measuring circuit takes a simple form assuming no losses:

$$\begin{gathered} I = \mathbf{E}_{out}^{+}\mathbf{E}_{out} = \frac{1}{4}\left(e^{i\beta_x L} + e^{i\beta_y L}\right)\cdot\left(e^{-i\beta_x L} + e^{-i\beta_y L}\right) = \frac{1}{4}\left(1 + e^{-i\left[\beta_x - \beta_y\right]L} + e^{i\left[\beta_x - \beta_y\right]L} + 1\right) = \\ = \frac{1}{4}\left(2 + 2\cos\left[\left(\beta_x - \beta_y\right)L\right]\right) = \frac{1}{2}\left(1 + \cos\left[\left(\beta_x - \beta_y\right)L\right]\right) \end{gathered} \tag{7}$$

Since the propagation constants depend on the wavelength, it is obvious that the output intensity (see Eq. (7)) also depends on the wavelength. In fact, this dependence can be considered the STF of the SFPI.

Next, we show that the beat length of fiber modes and, accordingly, its birefringence can be measured by Fourier analysis of this function.

STF of polarization interferometer taking into account polarization dispersion. Let us consider the technique for obtaining the Fourier transform of the STF defined by expression (7).

For further analysis, it is advisable to expand the propagation constants of the polarization modes into a Taylor series with respect to the wavelength λ, taking into account the linear terms of the expansion:

$$\beta_{x,y}(\lambda) = \frac{2\pi n_{x,y}(\lambda_0)}{\lambda_0} + 2\pi \cdot \frac{d}{d\lambda}\left(\frac{n_{x,y}(\lambda_0)}{\lambda}\right)_{\lambda_0} \cdot (\lambda - \lambda_0), \tag{8}$$

where λ_0 is the central wavelength of the Taylor series expansion.

In view of the derivative in expression (8), we obtain:

$$\beta_{x,y}(\lambda) = \frac{2\pi n_{x,y}(\lambda_0)}{\lambda_0} + \left[\frac{2\pi}{\lambda_0} \cdot \frac{dn_{x,y}(\lambda)}{d\lambda}\bigg|_{\lambda_0} - \frac{2\pi}{\lambda_0^2} \cdot n_{x,y}(\lambda_0) \right] \cdot (\lambda - \lambda_0). \quad (9)$$

The derivatives of the refractive indices of the modes with respect to the wavelength λ in expression (9) reflect the effect of polarization dispersion.

If we substitute expression (9) into Eq. (7), we obtain the expression for the intensity of light at the output of the SFPI as a function of wavelength:

$$I_{out}(\lambda) = A \cdot \left\{ 1 + \cos\left[L \cdot \left(\begin{array}{l} \dfrac{2\pi}{\lambda_0} \cdot (n_x^0 - n_y^0) - \\ -(\lambda - \lambda_0) \cdot \dfrac{2\pi}{\lambda_0^2} \left[(n_x^0 - n_y^0) - \lambda_0 \cdot \left(\dfrac{dn_x(\lambda)}{d\lambda}\bigg|_{\lambda_0} - \dfrac{dn_y(\lambda)}{d\lambda}\bigg|_{\lambda_0} \right) \right] \end{array} \right) \right] \right\}, \quad (10)$$

where $n_{x,y}^0$ are the refractive indices of the core for waves with polarizations $\mathbf{E}_{x,y}$ at a wavelength λ_0; A is the amplitude coefficient determined by the input radiation.

Expression (10) represents the STF of the SFPI taking into account the expansion of the propagation constants into a Taylor series and has the form of a harmonic function of the variation in light intensity at the output of the interferometer depending on the wavelength of the source by means of a multiplier $(\lambda - \lambda_0)$. Analysis of expression (10) allows to conclude that the presence of polarization dispersion changes the period of the STF. This statement will be proved below in the calculations.

Expression (10) can be used to estimate such a quantity as the beat length taking into account the polarization dispersion L_b^{gr}. Indeed, the beat length is the length of the fiber section at which the phase difference of polarization modes changes by 2π. In view of this and the condition for the change in the phase difference of the modes by 2π with a change in wavelength by $(\lambda - \lambda_0)$, the expressions for the beat length of the modes and birefringence, taking into account the polarization dispersion L_b^{gr}, can be written as follows:

$$L_b^{gr} = \frac{\lambda_0}{\Delta n_{x,y}^0 - \lambda_0 \cdot \left(\dfrac{dn_x}{d\lambda}|_{\lambda_0} - \dfrac{dn_y}{d\lambda}|_{\lambda_0} \right)} = \frac{\lambda_0}{B},$$
$$B = \Delta n_{x,y}^0 - \lambda_0 \cdot \left(\frac{dn_x}{d\lambda}|_{\lambda_0} - \frac{dn_y}{d\lambda}|_{\lambda_0} \right). \quad (11)$$

It follows from expressions (11) that the presence of polarization dispersion leads to a decrease in birefringence and an increase in the beat length. The superscript *gr* in L_b^{gr} reflects accounting for the group velocities of interfering polarization modes used to construct this quantity.

Since the phase difference of polarization modes changes during scanning of the wavelength λ, the beat length can evidently be estimated from the STF. In the case of linear variation in the optical frequency, the STF formed is a harmonic function. The change in the wavelength $\delta\lambda_b$ for which the phase difference of polarization modes changes by 2π corresponds to one period of the STF. This circumstance makes it possible to estimate the beat length by the period of the STF.

Indeed, taking into account the above, we can use expressions (10) and (11) to obtain the relations:

$$\frac{L}{L_b^{gr}} = \frac{\lambda_0}{\delta\lambda_b} \rightarrow L_b^{gr} = L \cdot \frac{\delta\lambda_b}{\lambda_0}, \quad (12)$$

where L is the length of the fiber considered.

Since L and λ_0 are known, the measurement of $\delta\lambda_b$ using STF allows to determine the beat length L_b^{gr} from Eq. (12).

It should be emphasized here that the spectral method introduces an additional parameter characterizing the PM fiber, which is $\delta\lambda_b$. As noted above, it is defined as the variation range of the light wavelength corresponding to one period of the STF. As seen from Eq. (12), this parameter also depends on other characteristics of the PM fiber. It primarily depends on the length of the fiber, as well as on its birefringence and dispersion included in expression (11) for the beat length of polarization modes. It is this parameter that is used to determine the beat length in coherent or incoherent spectral methods for measuring L_b [15]. In our study, this parameter was reasonably obtained by analyzing the Taylor series expansion of the propagation constants of polarization modes.

Analytical expression for Fourier transform of STF. Taking into account Eq. (12), expression (10) can be represented in a simpler form:

$$I(\lambda) = 1 + \cos\left[\Psi + \frac{2\pi L}{\lambda_0 L_b^{gr}}(\lambda - \lambda_0)\right], \tag{13}$$

where Ψ is a constant phase component independent of the wavelength λ and expressed as $\Psi = 2\pi \cdot n_{x,y}^0 \cdot L/\lambda_0$.

The Fourier-cosine transform of this expression has the form

$$\begin{aligned} S &= \sqrt{\frac{2}{\pi}} \int\limits_{-\frac{\Delta\lambda_{span}}{2}}^{\frac{\Delta\lambda_{span}}{2}} \cos\left[\Psi + \frac{2\pi L}{\lambda_0 L_b^{gr}}(\lambda - \lambda_0)\right] \cdot \cos(K \cdot \delta\lambda)\, d\delta\lambda = \\ &= \frac{1}{\sqrt{2\pi}} \int\limits_{-\frac{\Delta\lambda_{span}}{2}}^{\frac{\Delta\lambda_{span}}{2}} \cos\left[\delta\lambda(K_0 - K)\right] d\delta\lambda = \frac{1}{\sqrt{2\pi}} \cdot \frac{\sin\left[\Delta\lambda_{span}(K_0 - K)\right]}{\Delta\lambda_{span}(K_0 - K)}, \end{aligned} \tag{14}$$

where K_0 is a constant value for the given interferometer, $K_0 = \dfrac{2\pi \cdot L}{\lambda_0 \cdot L_b^{gr}}$; $\Delta\lambda_{span}$ is the wavelength scanning range; $\delta\lambda = \lambda - \lambda_0$; K is the wavelength-dependent argument in expression (14).

In view of Eqs. (12), the coefficients K and K_0 can be written as follows:

$$K_0 = \frac{2\pi \cdot L}{\lambda_0 \cdot L_b} = \frac{2\pi \cdot \lambda_0}{\lambda_0 \cdot \delta\lambda_b} = \frac{2\pi}{\delta\lambda_b}; K = \frac{2\pi}{\delta\lambda}.$$

Here and below, the superscript in the notation of the group beat length is omitted for simplicity.

Normalized expression (14) can be now written in the following form:

$$S(\delta\lambda) = \frac{\sin\left[2\pi\left(\dfrac{\Delta\lambda_{span}}{\delta\lambda_b} - \dfrac{\Delta\lambda_{span}}{\delta\lambda}\right)\right]}{2\pi\left(\dfrac{\Delta\lambda_{span}}{\delta\lambda_b} - \dfrac{\Delta\lambda_{span}}{\delta\lambda}\right)}, \tag{15}$$

where $\Delta\lambda_{span}$ is the wavelength scanning range, $\delta\lambda_b$ is the period of variation in STF intensity.

Expression (15) is actually the Fourier transform of the STF and depends only on two parameters: the scanning range $\Delta\lambda_{span}$ and the STF period $\delta\lambda_b$. Apparently, the function $S(\delta\lambda)$ has an extremum at $\delta\lambda = \delta\lambda_b$. Thus, the position of this extremum on the abscissa axis can be used to determine the STF period $\delta\lambda_b$ and the beat length of polarization modes:

$$L_b = L \cdot \frac{\delta\lambda_b}{\lambda_0}.$$

For further analysis, it is convenient to make the following substitutions:

$$N_0 = \frac{\Delta\lambda_{span}}{\delta\lambda_b},\ N = \frac{\Delta\lambda_{span}}{\delta\lambda}.$$

Eq. (15) then takes the form

$$S(N) = \frac{\sin\left[2\pi\left(N_0 - N\right)\right]}{2\pi\left(N_0 - N\right)}. \tag{16}$$

Let us interpret the meaning of the substitutions made during the transition from expression (15) to (16). The quantity N_0, as follows from its definition given in the previous paragraph, numerically corresponds to the number of STF periods in the wavelength scanning range $\Delta\lambda_{span}$. This implies a statement that is important for practical implementation of the approach under consideration: the application of the fast Fourier transform (FFT) to STF ensures that N_0 is found, since the numerical value of the sample on the abscissa corresponding to some spectral component of FFT characterizes the number of harmonic oscillation periods that fit in this sample.

Based on this, it is possible to formulate a simple algorithm for finding the beat length and birefringence of the fiber.

Step 1. Construct SFPI circuit containing an optical laser source with tunable wavelength (such as an interrogator with the required wavelength modulation range).

Step 2. Record the STF, subsequently applying the FFT to it.

Step 3. Determine the numerical value of the sample N_0 at which an extremum characterizing the interference of polarization modes is observed.

Step 4. Obtain the value of the beat length from expression (12), taking into account the substitution $N_0 = \Delta\lambda_{span}/\delta\lambda_b$, using the expression

$$L_b = \frac{L \cdot \Delta\lambda_{span}}{\lambda_0 \cdot N_0}.$$

Step 5. Estimate the birefringence value using expression (11) $\Delta n_{xy} \approx \frac{\lambda_0}{L_b}$.

Fig. 2 shows the STF and the corresponding Fourier transforms of the SFPI STF for three lengths of the fiber under study, obtained by Eqs. (10) and (16), respectively. The following values of calculation parameters were selected [29]:

$$\lambda_0 = 1550 \text{ nm}, \Delta\lambda_{span} = 80 \text{ nm},$$

$$n_x - n_y = 4.983 \cdot 10^{-4},$$

$$\frac{dn_x}{d\lambda} - \frac{dn_y}{d\lambda} = 3.2 \cdot 10^{-8}\ \frac{1}{\text{nm}}.$$

Evidently, as the length of the fiber under study increases, the period of the corresponding STF decreases proportionally and the spectral component in the Fourier transform shifts to the right on the abscissa, which corresponds to theoretical predictions. Fig. 2, *c, f* additionally shows the STFs and their Fourier transforms obtained for the case of absence of polarization dispersion. It

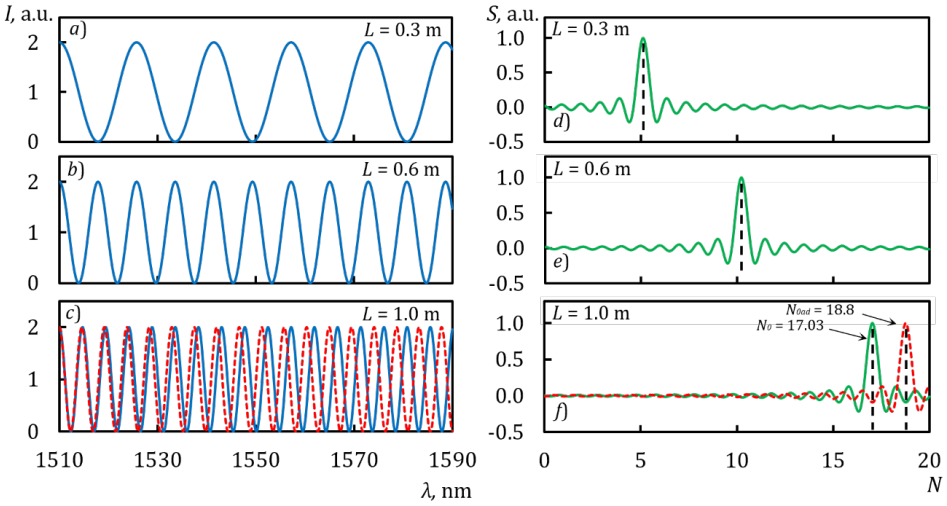

Fig. 2. SFPI STF (*a*–*c*) and corresponding Fourier transforms (*d*–*f*) for three lengths L of fiber under study. The STFs and the Fourier transform are also shown for absence of polarization dispersion (red dashed lines in (*c*) and (*g*));
N_0, N_{0ad} are the parameters expressing the coordinate of the maximum spectral component in the presence and absence of dispersion, respectively; the values of the calculation parameters are given in the text

can be seen that the presence of polarization dispersion leads to an increase in the STF period and a shift to the left on the abscissa of the corresponding spectral component (i.e., to an increase in the beat length).

We can find the beat length from the Fourier transforms shown in Fig. 2, *d*–*f* as

$$L_b^{gr} = \frac{L \cdot \Delta\lambda_{span}}{\lambda_0 \cdot N_0}.$$

The beat length for all three cases $L_b^{gr} = 3$ mm. This corresponds to theoretical predictions, since the beat length of the fiber does not depend on its length. Accordingly, birefringence $\Delta n_{xy} \approx \lambda_0 / L_b^{gr} = 10 \cdot 5.11^{-4}$.

Similar calculations of the beat length and birefringence yielded results of 2.75 mm and $5.65 \cdot 10^{-4}$, respectively, for the case of absence of dispersion (red dashed line in Fig. 2,*f*). Thus, the presence of polarization dispersion leads to an increase in the beat length and a decrease in birefringence, which corresponds to theoretical predictions.

This section presents a model of the SFPI taking into account the polarization dispersion. It is shown that the approach aimed at obtaining the Fourier transform of the STF makes it possible to effectively determine the beat length of the fiber under study. It is also established that the developed model makes it possible to evaluate the effect of polarization dispersion on fiber birefringence.

Analysis of the effect of angular misalignment between the birefringence axes of the fiber under study and the axes of the input and output fibers. Analysis of expressions (5)–(7) shows that the optimal mode of SFPI operation is achieved in the case of orientation of the axes of the fiber under study at an angle $\psi_{1,2} = 45^\circ$ relative to the axes of the input and output fibers, since in this case the orthogonal polarization modes in the fiber have equal amplitudes.

However, these angles may deviate from the values $\psi_{1,2} = 45^\circ$ in the practical implementation of the SFPI circuit, due to the inevitable errors occurring during assembly of the interferometer and splicing of optical fibers. In view of this, we deemed it necessary to conduct analytical review of the case of angular misalignment to determine its effect on the SFPI signal.

The complete Jones matrix for the case of arbitrary values of angles $\psi_{1,2}$ has the following form:

$$W_{\Sigma} = \begin{pmatrix} 0 & 0 \\ 0 & 1 \end{pmatrix} \cdot \begin{pmatrix} e^{-i(\beta_x L)_2} & 0 \\ 0 & e^{-i(\beta_y L)_2} \end{pmatrix} \cdot \begin{pmatrix} \cos\psi_2 & \sin\psi_2 \\ -\sin\psi_2 & \cos\psi_2 \end{pmatrix} \cdot \begin{pmatrix} e^{-i\beta_x L} & 0 \\ 0 & e^{-i\beta_y L} \end{pmatrix} \times$$
$$\times \begin{pmatrix} \cos\psi_1 & -\sin\psi_1 \\ \sin\psi_1 & \cos\psi_1 \end{pmatrix} \cdot \begin{pmatrix} e^{-i(\beta_x L)_1} & 0 \\ 0 & e^{-i(\beta_y L)_1} \end{pmatrix}, \quad (17)$$

where $(\beta_{x,y} \cdot L)_1$ and $(\beta_{x,y} \cdot L)_2$ correspond to the additional input and output fibers necessary for plugging optical connectors and included in the SFPI circuit, respectively.

Then the output Jones vector takes the form:

$$E_{out} = e^{-i\left[(\beta_y L)_1 + (\beta_y L)_2\right]} \cdot \begin{pmatrix} 0 \\ \sin\psi_2 \cdot \sin\psi_1 \cdot e^{-i\beta_x L} + \cos\psi_2 \cdot \cos\psi_1 \cdot e^{-i\beta_y L} \end{pmatrix}. \quad (18)$$

It can be seen from expression (18) that the parameters of the input and output fibers are contained in the phase multiplier in front of the Jones vector. Evidently, these parameters should not affect the output intensity.

Thus, the intensity of the light entering the photodetector can be written as follows:

$$I = E_{out}^{+} \cdot E_{out} = \cos^2(\psi_2) - \cos 2\psi_2 \sin^2(\psi_1) + \frac{1}{2} \cdot \sin 2\psi_2 \cdot \sin 2\psi_1 \cdot \cos\left[(\beta_x - \beta_y) L\right]. \quad (19)$$

Specifically, the contrast and the constant component of the interference signal are functions of the splicing angles between the fiber under study and the input and output fibers.

The contrast of the signal V and the constant component I_c can be written as

$$V = \frac{\sin 2\psi_2 \cdot \sin 2\psi_1}{2 \cdot \left[\cos^2(\psi_2) - \cos 2\psi_2 \sin^2(\psi_1)\right]}, \quad (20)$$

$$I_c = \cos^2(\psi_2) - \cos 2\psi_2 \sin^2(\psi_1). \quad (21)$$

Fig. 3 shows the calculation results for the contrast of the interference signal V and the constant component I_c depending on the angle ψ_1 for three values of the angle ψ_2 using Eqs. (20) and (21), respectively. It can be seen that the contrast is maximum in the absence of misalignment (angles $\psi_{1,2} = °45$), and the constant component is equal to half the maximum intensity of the interference signal. If the angles $\psi_{1,2}$ deviate from 45°, variations in contrast and the constant component are observed.

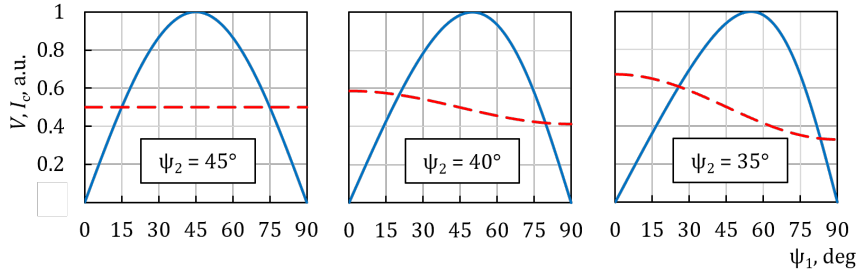

Fig. 3. Dependences of contrast of interference signal V (blue solid lines) and constant component I_c (red dashed lines) on the angle ψ_1 for three values of the angle ψ_2

Analysis of the effect of angular misalignment between the axes of fiber polarizers and connected fibers. Let us consider another case that is important for practice, when there is angular misalignment between the axes of fiber polarizers and the fibers connected to them. In such a situation, the Jones matrix of the entire system has a significantly more complex form. To simplify the expressions, let us assume that the misalignment only appears in the segment with the first polarizer and the input fiber. In other words, a linear state of polarization is observed at the input to the circuit, but its orientation does not coincide with any of the axes of the first fiber and the misalignment angle is equal to α. Then the output intensity of the SFPI is determined by the expression

$$I = \frac{1}{2}\cdot\left\langle \begin{array}{l} 1-\cos 2\alpha\cdot\left\{\begin{array}{l}\cos 2\Psi_1\cdot\cos 2\Psi_2+\\ +\sin 2\Psi_1\cdot\sin 2\Psi_2\cdot\cos\left[\left(\beta_x-\beta_y\right)L\right]\end{array}\right\}+ \\ +\sin 2\alpha\cdot\left\{\begin{array}{l}\cos 2\Psi_1\cdot\sin 2\Psi_2\cdot\cos\left[\left(\beta_{x1}-\beta_{y1}\right)L_1\right]+\\ +\sin 2\Psi_1\cdot\sin^2\left(\Psi_2\right)\cdot\cos\left[\left(\beta_x-\beta_y\right)L-\left(\beta_{x1}-\beta_{y1}\right)L_1\right]-\\ -\sin 2\Psi_1\cdot\cos^2\left(\Psi_2\right)\cdot\cos\left[\left(\beta_x-\beta_y\right)L+\left(\beta_{x1}-\beta_{y1}\right)L_1\right]\end{array}\right\} \end{array}\right\rangle, \qquad (22)$$

where the parameters with the subscript 1 refer to the first fiber (L_1), the parameters without subscripts (L) refer to the PM fiber under study.

Expression (22) contains a constant component (1st line); a harmonic that defines the birefringence of the fiber under study (2nd line); a harmonic that defines the PM fiber at the input to the SFPI circuit, i.e., the first (input) optical fiber (3rd line). Additionally, combination frequencies are present, the difference (4th line) and total (5th line) harmonics.

Note that in this configuration of the circuit, the amplitudes of all the components in Eq. (22) depend on the misalignment angle α. In addition, in contrast to the misalignment in the splices, 'parasitic' combination components with birefringence that do not correspond to the birefringence of the fiber measured appear in this case. All parasitic components disappear at an angle $\alpha = 0°$.

Fig. 4, *a*–*c* shows the SPFs, i.e., the dependences of the intensity of the interference signal I on the wavelength λ, obtained in accordance with expression (22) for three values of the misalignment angle α and the optimal angles corresponding to the orientation of the axes of the fiber under study $\psi_{1,2} = °45$. Fig. 4, *d*–*f* shows the corresponding Fourier transforms of these dependences obtained by applying FFT to the corresponding STFs.

Similar calculations by Eq. (22) were performed at a fixed angle $\alpha = 10°$ and different angles ψ_1 and ψ_2 (Fig. 5).

Evidently, in the absence of misalignment ($\alpha = 0°$, $\psi_1 = \psi_2 = 45°$), the dependence of the intensity of the interference signal I on the wavelength λ is a harmonic function (see Fig. 4, *a*, *d*). The presence of angular misalignment ($\alpha = 10°$ and 20є) leads to the appearance of additional harmonics, distortion of the waveform and a decrease in contrast (see Figs. 4, *b*, *c* and 5, *a*–*h*). Importantly, the estimation of the period of interference signal $I(\lambda)$ in the presence of angular misalignment may turn out to be erroneous because it is impossible to accurately determine the period of the interference component corresponding to the principal pair of polarization modes. However, the period of this component can be estimated more accurately if the Fourier transform of the interference signal is used. This is exactly the approach proposed in this paper.

To summarize, we analyzed the dependences of STF on the misalignment angle in the SFPI circuit. It is shown that the deviation of the splicing angles $\psi_{1,2}$ from the value of 45° leads to a decrease in the contrast of the interference signal. It is also shown that when the polarization orientation of the input radiation is misaligned with the axes of the input fiber, the birefringence deviates from the harmonic, and additional harmonics appear in its Fourier transform. Due to the appearance of additional harmonics, the estimation of the beat length of the fiber under study through direct measurement of the period of the interference signal may yields errors. To avoid such errors associated with the presence of additional harmonics, we propose using Fourier analysis of the interference signal, which allows to more accurately estimate the period of the spectral component corresponding to the interference of a pair of principal polarization modes.

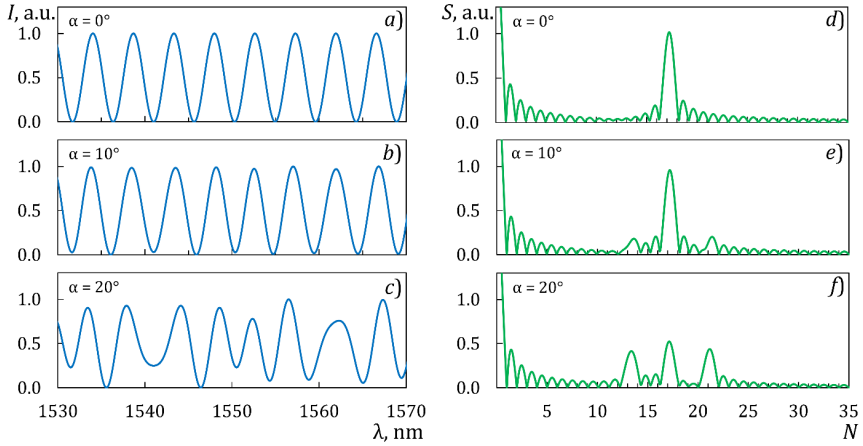

Fig. 4. STF (*a*–*c*) and corresponding Fourier transforms (*d*–*f*) for three cases of angle α characterizing the misalignment of the input polarizer axis with the birefringence axes, at the same orientation angles of the birefringence axes of the fiber under study: $\psi_1 = \psi_2 = 45°$

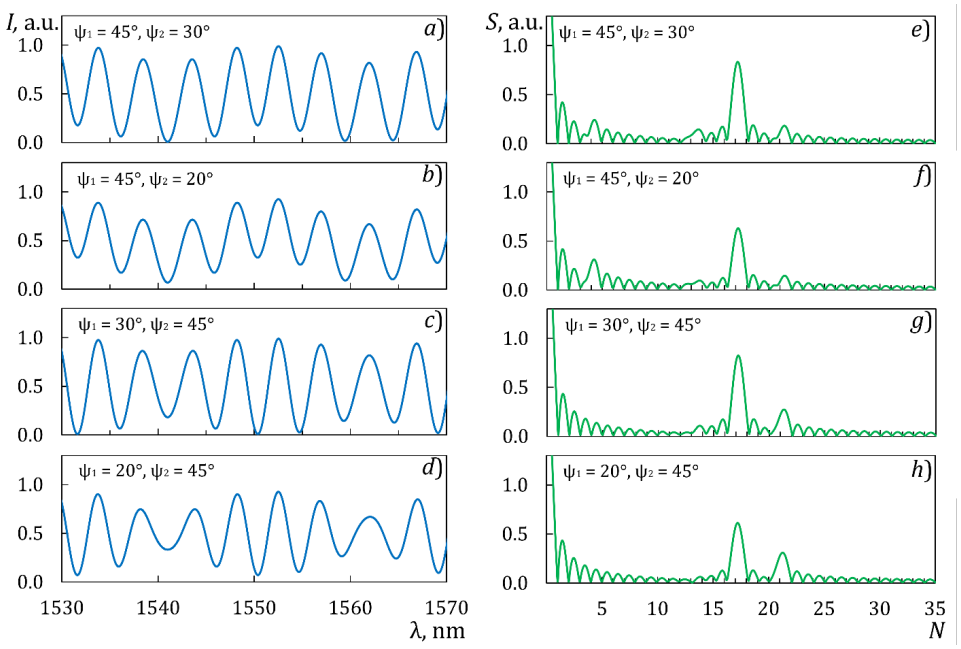

Fig. 5. SPF (*a*–*d*) and corresponding Fourier transforms (*e*–*h*) for four orientation angles of the birefringence axes of the fiber under study at the same misalignment angles α (α = 10°) between the axis of the input polarizer with the birefringence axes

Experimental studies of PM fibers by the spectral method

Circuit for measuring the parameters of PM fibers. To measure the necessary parameters, we used a scanning laser and a photodetector synchronized with it, included in the NI PXIe-4844 interrogator. The scans were performed with sawtooth phase modulation with the following parameters.

Scanning parameter	**Parameter value**
Frequency, cycle/s	10
Optical power, MW	0.06
Central emission wavelength, nm	1550
Range, nm	1510–1590 ($\Delta\lambda_{span}$ = 80 nm)
Optical frequency band, THz	10
Step, pm	4 (0.5 GHz).

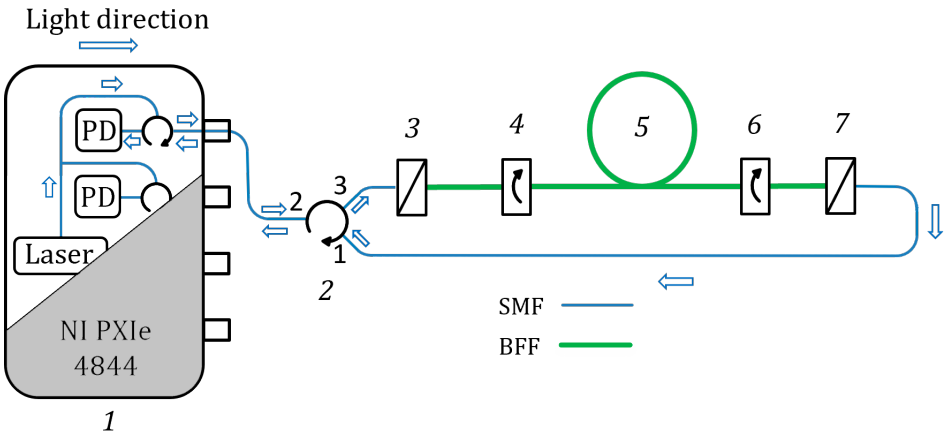

Fig. 6. Scheme of experimental setup for measurements by the spectral method (arrows indicate the direction of light propagation):
NI PXIe-4844 interrogator *1* (PD is the photodiode); optical circulator *2*; fiber-optic polarizers *3*, *7*; elements *4*, *6* for rotating the axes of the PM fiber by 45°; fiber *5*

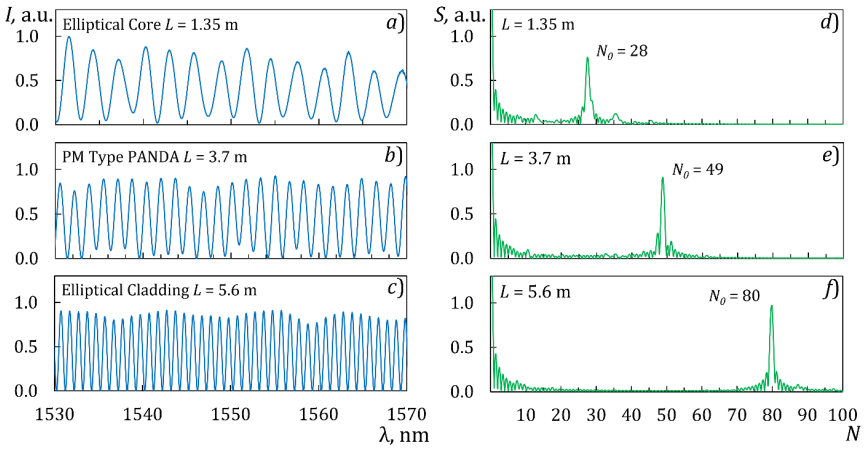

Fig. 7. Experimentally obtained STFs (*a*–*c*) and their Fourier transforms (*d*–*f*) for fibers of three types: with elliptical core (*a, d*), with elliptical stress-inducing cladding (*c, f*) and PANDA type (*b, e*)

Fig. 6 shows the measuring setup for studying PM fibers using the spectral method.

Measurement technique and results. The measurements were carried out by the technique described above. The light from the laser source first passes through a fiber-optic polarizer, then through a piece of fiber spliced at an angle $\psi = 45°$ to the principal axes, and then enters the fiber measured. To obtain an interference pattern, the light again passes through the optical element rotating the axes by 45° and the fiber-optic polarizer. Next, the output signal is sent through the circulator to the photodetector synchronized with the source.

Fig. 7, *a*–*c* shows experimentally obtained STFs and Fig. 7, *d*–*f* shows their Fourier transforms for the three types of fibers under study. A technique known in digital signal processing was used to increase the resolution of Fourier transforms [31]: before applying FFT, an array consisting of zeros was added to the numerical array corresponding to the STF.

It can be seen from Fig. 7, *a*–*c* shows that the two polarization components formed an STF during interference, which is a quasi-harmonic signal with one dominant spectral component. The obtained STF data can be used to acquire the necessary information about the required beat length parameter by two simple methods.

Method I. The experimental data can be used to find $\delta\lambda_b$, and then the formula $\frac{L_b}{L} = \frac{\delta\lambda_b}{\lambda_0}$ can be used to obtain the beat length:

$$L_b = \frac{L \cdot \delta\lambda_b}{\lambda_0}.$$

This approach is equivalent to the method of incoherent excitation of PM fiber using an optical spectrum analyzer [15].

Method II. It is based on the Fourier analysis method of STFs proposed in this paper. The FFT is applied to detected STFs. The value of the parameter N_0 expressing the coordinate of the maximum spectral component is found from the obtained Fourier transforms. Next, the beat length is found by the following formula:

$$L_b = \frac{L}{\lambda_0} \cdot \frac{\Delta\lambda_{span}}{N_0}.$$

The beat lengths obtained by the first and second methods are evidently the same in order of magnitude. However, the approach proposed in this paper involving Fourier analysis of the STFs provides more accurate results in cases when the form of the STF deviates from the harmonic due to unavoidable misalignment in the optical circuit.

The obtained characteristics of the studied PM fibers with different types of birefringence and different lengths are given in Table.

Table

Experimentally obtained characteristics of PM fibers

Fiber type	L, m	N	L_b, mm	B, 10^{-4}
PANDA	3.70	48		
	5.70	74	3.97	3.9
Elliptical stress cladding	5.60	80	3.61	4.3
	7.50	104	3.72	4.2
Elliptical core	1.35	28	2.53	6.1

Notations: L is the fiber length, N is the number of STF periods in the wavelength scan ning range $\Delta\lambda_{span}$, L_b is the beat length, B is the birefringence.

The results presented in this paper for the beat lengths obtained in experiments and calculations are in good agreement with the parameters of commercial PM fibers and with the results obtained by other authors [30] for this optical spectral range. For example, the beat length of PANDA-type PM fibers turned out to be 3.97 mm, which is in good agreement with the specifications for commercial fibers (3–5 mm).

Conclusion

The article presents a detailed theoretical and experimental study of a double spectral method for measuring the parameters of anisotropic optical fibers with linear birefringence taking into account the dispersion of refractive indices.

The section "Theoretical analysis" considers a polarization fiber interferometer as an integral part of the optical measuring system. We obtained expressions for the main characteristics of the interferometer taking into account the effect of dispersion, that is, the spectral transfer function and its Fourier transform, deriving expressions for birefringence and the beat length of modes based on these characteristics. For this purpose, we used the Taylor series expansion of the propagation constants of polarization modes with respect to the wavelength, allowing to account for the effect of mode dispersion.

In addition, the Jones matrix method was used to comprehensively analyze the effect of misalignment between the angles of various fiber elements in the optical circuit on the key parameters of the polarization interferometer. It is established that a deviation from the optimal angle of 45° in the device rotating the axes of the PM fiber causes a decrease in the contrast of the interference pattern. The angular misalignment of the input PM fiber produces parasitic interference signals with combination birefringence values. Model calculations were performed for the characteristics of PM fibers, making it possible to accurately estimate the main parameters of anisotropic optical fibers.

The section «Experimental studies...» describes a measuring circuit using an interrogator and signal processing methods. The spectral transfer functions of PM fibers and their Fourier transforms are given. The spectral method was used in experiments with three types of birefringent fibers:

PANDA-type,

with elliptical stress-cladding,

with elliptical core.

The samples differed by length and magnitude of birefringence. Spectral transfer functions, their Fourier transforms, beat lengths, and birefringence values are obtained for each of them. Where possible, the characteristics provided by the manufacturer were compared with experimental results related to PANDA-type optical fibers and optical fibers with an elliptical core; as a result, their good agreement was obtained.

REFERENCES

1. **Fokin V. G.,** Kogerentnye opticheskie seti [Coherent optical networking], Published by Siberian State University of Telecommunications & Information Sci., Novosibirsk, 2015 (in Russian).

2. **Betti S., De Marchis G., Iannone E.,** Coherent optical communications systems (Wiley Series in Microwave and Optical Engineering), Wiley-Interscience, New York, 1995.

3. **Tian S., Tang Y., Zhang Y., et al.,** Simultaneous measurement of strain and temperature based on dual cross-axis interference polarization-maintaining fiber interferometer, J. Light. Technol. 40 (14) (2022) 4878–4885.

4. **Leandro D., Lopez-Amo M.,** All-PM fiber loop mirror interferometer analysis and simultaneous measurement of temperature and mechanical vibration, J. Light. Technol. 36 (4) (2018) 1105–1111.

5. **Sasaki K., Takahashi M., Hirata Y.,** Temperature-insensitive Sagnac-type optical current transformer, J. Light. Technol. 33 (12) (2015) 2463–2467.

6. **Liu J., Liu Y., Xu T.,** Bias error and its thermal drift due to fiber birefringence in interferometric fiber-optic gyroscopes, Opt. Fiber Technol. 55 (March) (2020) 102138.

7. **Pang F., Zheng H., Liu H., et al.,** The orbital angular momentum fiber modes for magnetic field sensing, IEEE Photonics Technol. Lett. 31 (11) (2019) 893–896.

8. **Abdulhalim I., Gannot I., Pannell C. N.,** All-fiber and fiber compatible acousto-optic modulators with potential biomedical applications, Proc. SPIE. 6083 (15 Febr) (2006) 60830K.

9. **Payne D. N., Barlow A. J., Hansen J. J. R.,** Development of low- and high-birefringence optical fibers, IEEE J. Quantum Electron. 18 (4) (1982) 477–488.

10. **Filippov V. N., Kotov O. I., Nikolayev V. M.,** Measurement of polarization beat length in single-mode optical fibres with a polarization modulator, Electron. Lett. 26 (10) (1990) 658–660.

11. **Calvani R., Caponi R., Cisternino F., Coppa G.,** Method of measuring polarization and birefringence in single-mode optical fibers. Patent No. US-4866266-A, Assignee: Cselt Centro Studi Lab Telecom (IT), United States. Priority: 1987/05/20. Grant: 1989/09/12.

12. **Kim B. Y., Choi S. S.,** Analysis and measurement of birefringence in single-mode fibers using the backscattering method, Opt. Lett. 6 (11) (1981) 578–580.

13. **Nakazawa M., Horiguchi T., Tokuda M., Uchida N.,** Polarization beat length measurement in a single-mode optical fiber by backward Rayleigh scattering, Electron. Lett. 17 (15) (1981) 513–515.

14. **Ross J. N.,** Birefringence measurement in optical fibers by polarization optical-timedomain reflectometry, Appl. Opt. 21 (19) (1982) 3489–3495.

15. **Morshnev S. K., Gubin V. P., Starostin N. I., et al.,** Beat length measurement optical fibers, Photonics Russia. 12 (6(74)) (2018) 616–633.

16. **Ibrahim S. K., Farnan M., Karabacak D. M.,** Design of a photonic integrated based optical interrogator, Proc. SPIE. 10110 (20 Febr.) Photonic Instrumentation Engineering IV (2017) 241–249.

17. **Mikhailov S., Matthes A., Bierlich J., et al.,** Highly birefringent microstructured optical fiber for distributed hydrostatic pressure sensing with sub-bar resolution, Opt. Express. 30 (11) (2020) 19961–19973.

18. **Urbanczyk N., Szpulak M., Statkiewicz-Barabach G., et al.,** Sensing capabilities of the birefringent holey fibers, Proc. the 6th Int. Conf. on Transparent Optical Networks, Wroclaw, Poland; Aug, 2004, IEEE. (IEEE Cat. No. 04EX804), 2 (2004) 91–94.

19. **Eronyan M. A., Devetyarov D. R., Reutskiy A. A., et al.,** Polarization-maintaining and radiation resistant optical fiber with germanosilicate optical core, Opt. Fiber Technol. 68 (Jan) (2022) 102789.

20. **Xu S., Shao H., Li Ch., et al.,** A linear birefringence measurement method for an optical fiber current sensor, Sensors. 17 (7) (2017) 1556.

21. **Cao S., Xie S., Zhang M.,** Polarization beat length estimation based on the statistical properties of Brillouin gain in SMF, IEEE Photon. Technol. Lett. 28 (18) (2016) 1960–1963.

22. **Petrov A. V., Chapalo I. E., Bisyarin M. F., Kotov O. I.,** Intermodal fiber interferometer based on broadband light source and optical spectrum analyzer for external perturbations measurement, Pisma v Zhurnal Tekhnicheskoi Fiziki. 47 (23) (2021) 8–11 (in Russian).

23. **Petrov A. V., Chapalo I. E., Bisyarin M. F., Kotov O. I.,** Intermodal fiber interferometer with frequency scanning laser for sensor application, Appl. Opt. 59 (33) (2020) 10422–10431.

24. **Eickhoff W., Yen Y., Ulrich R.,** Wavelength dependence of birefringence in single-mode fiber, Appl. Opt. 20 (19) (1981) 3428–3435.

25. **Rashleigh S. C.,** Wavelength dependence of birefringence in highly birefringent fibers, Opt. Lett. 7 (8) (1982) 294–296.

26. **Barlow A., Payne D.,** The stress-optic effect in optical fibers, IEEE J. Quantum Electron. 19 (5) (1983) 834–839.

27. **Yariv A., Yeh P.,** Optical waves in crystals: propagation and control of laser radiation (Wiley Series in Pure and Applied Optics), John Wiley & Sons, New York, 1984.

28. **Temkina V. S., Liokumovich L.B., Archelkov A. B., et al.,** Description of polarization-maintaining fibers in analyzing the practical fiber-optic circuits using the Jones formalism, St. Petersburg State Polytechnical University Journal. Physics and Mathematics. 16 (3) (2023) 95–114 (in Russian).

29. **Liu J., Liu Y., Xu T.,** Analytical estimation of stress-induced birefringence in Panda-type polarization-maintaining fibers, IEEE Photon. Technol. Lett. 32 (24) (2020) 1507–1510.

30. **Andreev A. G., Bureev S. V., Eron'yan M. A., et al.,** Increasing the birefringence in anisotropic single-mode fiber lightguides with an elliptical stress cladding, J. Opt. Technol. 79 (9) (2012) 608–609.

31. **Sergienko A. B.** Tsifrovaya obrabotka signalov [Digital signal processing], "Peter" Publishing House, St. Petersburg, 2007 (in Russian).

СПИСОК ЛИТЕРАТУРЫ

1. **Фокин В. Г.** Когерентные оптические сети. Новосибирск: Изд. СибГУТИ, 2015. 372 с.

2. **Betti S., De Marchis G., Iannone E.** Coherent optical communications systems (Wiley Series in Microwave and Optical Engineering). New York: Wiley-Interscience, 1995. 539 p.

3. **Tian S., Tang Y., Zhang Y., et al.** Simultaneous measurement of strain and temperature based on dual cross-axis interference polarization-maintaining fiber interferometer // Journal of Lightwave Technology. 2022. Vol. 40. No. 14. Pp. 4878–4885.

4. **Leandro D., Lopez-Amo M.** All-PM fiber loop mirror interferometer analysis and simultaneous measurement of temperature and mechanical vibration // Journal of Lightwave Technology. 2018. Vol. 36. No. 4. Pp. 1105–1111.

5. **Sasaki K., Takahashi M., Hirata Y.** Temperature-insensitive Sagnac-type optical current transformer // Journal of Lightwave Technology. 2015. Vol. 33. No. 12. Pp. 2463–2467.

6. **Liu J., Liu Y., Xu T.** Bias error and its thermal drift due to fiber birefringence in interferometric fiber-optic gyroscopes // Optical Fiber Technology. 2020. Vol. 55. March. P. 102138.

7. **Pang F., Zheng H., Liu H., Yang J., Chen N., Shang J., Ramachandran S., Wang T.** The orbital angular momentum fiber modes for magnetic field sensing // IEEE Photonics Technology Letters. 2019. Vol. 31. No. 11. Pp. 893–896.

8. **Abdulhalim I., Gannot I., Pannell C. N.** All-fiber and fiber compatible acousto-optic modulators with potential biomedical applications // Proceedings of SPIE. 2006. Vol. 6083. 15 February. P. 60830K.

9. **Payne D. N., Barlow A. J., Hansen J. J. R.** Development of low- and high-birefringence optical fibers // IEEE Journal of Quantum Electronics. 1982. Vol. 18. No. 4. Pp. 477–488.

10. **Filippov V. N., Kotov O. I., Nikolayev V. M.** Measurement of polarization beat length in single-mode optical fibres with a polarization modulator // Electronics Letters. 1990. Vol. 26. No. 10. Pp. 658–660.

11. **Calvani R., Caponi R., Cisternino F., Coppa G.** Method of measuring polarization and birefringence in single-mode optical fibers. Patent No. US-4866266-A. Assignee: Cselt Centro Studi Lab Telecom (IT), United States. Priority: 1987/05/20. Grant: 1989/09/12.

12. **Kim B. Y., Choi S. S.** Analysis and measurement of birefringence in single-mode fibers using the backscattering method // Optics Letters. 1981. Vol. 6. No. 11. Pp. 578–580.

13. **Nakazawa M., Horiguchi T., Tokuda M., Uchida N.** Polarization beat length measurement in a single-mode optical fiber by backward Rayleigh scattering // Electronics Letters. 1981. Vol. 17. No. 15. Pp. 513–515.

14. **Ross J. N.** Birefringence measurement in optical fibers by polarization optical-timedomain reflectometry // Applied Optics. 1982. Vol. 21. No. 19. Pp. 3489–3495.

15. **Моршнев С. К., Губин В. П., Старостин Н. И., Пржиялковский Я. В., Сазонов А. И.** Измерение длины биений в двулучепреломляющих волоконных световодах // Фотоника. 2018. Т. 12. № 6 (74). С. 616–633.

16. **Ibrahim S. K., Farnan M., Karabacak D. M.** Design of a photonic integrated based optical interrogator // Proceedings of SPIE. 2017. Vol. 10110. Photonic Instrumentation Engineering IV. 20 February. Pp. 241–249.

17. **Mikhailov S., Matthes A., Bierlich J., Kobelke J., Wondraczek K., Berghmans F., Geernaert T.** Highly birefringent microstructured optical fiber for distributed hydrostatic pressure sensing with sub-bar resolution // Optics Express. 2022. Vol. 30. No. 11. Pp. 19961–19973.

18. **Urbanczyk N., Szpulak M., Statkiewicz-Barabach G., Martynkien T., Olszewski J.** Sensing capabilities of the birefringent holey fibers // Proceedings of the 6th International Conference on Transparent Optical Networks. Wroclaw, Poland, August, 2004. IEEE, 2004. (IEEE Cat. No. 04EX804). Vol. 2. Pp. 91–94.

19. **Eronyan M. A., Devetyarov D. R., Reutskiy A. A., Untilov A. A., Aksarin S. M., Meshkovskiy I. K., Bisyarin M. A., Pechenkin A. A.** Polarization-maintaining and radiation resistant optical fiber with germanosilicate optical core // Optical Fiber Technology. 2022. Vol. 68. January. P. 102789.

20. **Xu S., Shao H., Li Ch., Xing F., Wang Y., Li W.** A linear birefringence measurement method for an optical fiber current sensor // Sensors. 2017. Vol. 17. No. 7. P. 1556.

21. **Cao S., Xie S., Zhang M.** Polarization beat length estimation based on the statistical properties of Brillouin gain in SMF // IEEE Photonics Technology Letters. 2016. Vol. 28. No. 18. Pp. 1960–1963.

22. **Петров А. В., Чапало И. Е., Бисярин М. А., Котов О. И.** Межмодовый волоконный интерферометр на основе широкополосного источника света и анализатора оптического спектра для измерения внешних воздействий // Письма в Журнал технической физики. 2021. Т. 47. № 23. С. 8–11.

23. **Petrov A. V., Chapalo I. E., Bisyarin M. F., Kotov O. I.** Intermodal fiber interferometer with frequency scanning laser for sensor application // Applied Optics. 2020. Vol. 59. No. 33. Pp. 10422–10431.

24. **Eickhoff W., Yen Y., Ulrich R.** Wavelength dependence of birefringence in single-mode fiber // Applied Optics. 1981. Vol. 20. No. 19. Pp. 3428–3435.

25. **Rashleigh S. C.** Wavelength dependence of birefringence in highly birefringent fibers // Optics Letters. 1982. Vol. 7. No. 8. Pp. 294–296.

26. **Barlow A., Payne D.** The stress-optic effect in optical fibers // IEEE Journal of Quantum Electronics. 1983. Vol. 19. No. 5. Pp. 834–839.

27. **Ярив А., Юх П.** Оптические волны в кристаллах. Пер. с англ. М.: Мир, 616 .1987 с.

28. **Темкина В. С., Лиокумович Л. Б., Арчелков А. Б., Бучилко И. Р., Медведев А. В., Петров А. В.** Описание волоконных световодов с линейным двулучепреломлением при анализе практических оптоволоконных схем методом векторов и матриц Джонса // Научно-технические ведомости СПбГПУ. Физико-математические науки. 2023. Т. 16. № 3. С. 95–114.

29. **Liu J., Liu Y., Xu T.** Analytical estimation of stress-induced birefringence in Panda-type polarization-maintaining fibers // IEEE Photonics Technology Letters. 2020. Vol. 32. No. 24. Pp. 1507–1510.

30. **Андреев А. Г., Буреев С. В., Ероньян М. А., Комаров А. В., Крюков И. И., Мазунина Т. В., Полосков А. А., Тер-Нерсесянц Е. В., Цибиногина М. К.** Повышение двулучепреломления в анизотропных волоконных световодах с эллиптической напрягающей оболочкой // Оптический журнал. 2012. Т. 79. № 9. С. 107–109.

31. **Сергиенко А. Б.** Цифровая обработка сигналов. СПб.: Питер, 2007. 751 с.

THE AUTHORS

GOLOVCHENKO Andrew I.
Peter the Great St. Petersburg Polytechnic University
29 Politechnicheskaya St., St. Petersburg, 195251, Russia
golovchenko.ai@edu.spbstu.ru
ORCID: 0009-0005-9699-8497

PETROV Aleksandr V.
Peter the Great St. Petersburg Polytechnic University
29 Politechnicheskaya St., St. Petersburg, 195251, Russia
petrov.av1@spbstu.ru
ORCID: 0000-0001-5216-6588

TEMKINA Valentina S.
Peter the Great St. Petersburg Polytechnic University
29 Politechnicheskaya St., St. Petersburg, 195251, Russia
temkina_vs@spbstu.ru
ORCID: 0000-0003-2083-8989

ARCHELKOV Arseniy B.
Peter the Great St. Petersburg Polytechnic University
29 Politechnicheskaya St., St. Petersburg, 195251, Russia
arsarch11@gmail.com
ORCID: 0009-0007-4713-1293

TSIBINOGINA Marina K
Concern CSRI Elektropribor, JSC
30 Malaya Posadskaya St., St. Petersburg, 197046, Russia
cmk_07@mail.ru
ORCID: 0000-0003-2300-084X

KOTOV Oleg I.
Peter the Great St. Petersburg Polytechnic University
29 Politechnicheskaya St., St. Petersburg, 195251, Russia
kotov@rphf.spbstu.ru
ORCID: 0000-0001-8448-2024

СВЕДЕНИЯ ОБ АВТОРАХ

ГОЛОВЧЕНКО Андрей Игоревич – *аспирант Высшей школы прикладной физики и космических технологий Санкт-Петербургского политехнического университета Петра Великого.*
195251, Россия, г. Санкт-Петербург, Политехническая ул., 29
golovchenko.ai@edu.spbstu.ru
ORCID: 0009-0005-9699-8497

ПЕТРОВ Александр Викторович – *кандидат физико-математических наук, доцент Высшей школы прикладной физики и космических технологий Санкт-Петербургского политехнического университета Петра Великого.*
195251, Россия, г. Санкт-Петербург, Политехническая ул., 29
petrov.av1@spbstu.ru
ORCID: 0000-0001-5216-6588

ТЕМКИНА Валентина Сергеевна – *старший преподаватель Высшей школы прикладной физики и космических технологий Санкт-Петербургского политехнического университета Петра Великого.*
195251, Россия, г. Санкт-Петербург, Политехническая ул., 29
temkina_vs@spbstu.ru
ORCID: 0000-0003-2083-8989

АРЧЕЛКОВ Арсений Борисович – *студент Института электроники и телекоммуникаций Санкт-Петербургского политехнического университета Петра Великого.*
195251, Россия, г. Санкт-Петербург, Политехническая ул., 29
arsarch11@gmail.com
ORCID: 0009-0007-4713-1293

ЦИБИНОГИНА Марина Константиновна – *кандидат химических наук, ведущий инженер ОАО, концерна "ЦНИИ «Электроприбор»".*
197046, Россия, г. Санкт-Петербург, Малая Посадская ул., 30.
cmk_07@mail.ru
ORCID: 0000-0003-2300-084X

КОТОВ Олег Иванович – *доктор физико-математических наук, профессор Высшей школы прикладной физики и космических технологий Санкт-Петербургского политехнического университета Петра Великого.*
195251, Россия, г. Санкт-Петербург, Политехническая ул., 29
kotov@rphf.spbstu.ru
ORCID: 0000-0001-8448-2024

Received 05.09.2024. Approved after reviewing 17.09.2024. Accepted 24.10.2024.
Статья поступила в редакцию 05.09.2024. Одобрена после рецензирования 17.09.2024. Принята 24.10.2024.